# Optical imaging of coexisting collinear and spiral spin phases in the magnetoelectric multiferroic $MnWO_4$

Kouji Taniguchi,* Mitsuru Saito, and Taka-hisa Arima
*Institute of Multidisciplinary Research for Advanced Materials, Tohoku University, Sendai 980-8577, Japan*
(Received 4 November 2009; published 8 February 2010)

Optical absorption spectra of a magnetoelectric multiferroic $MnWO_4$ have been measured. It has been observed that the optical absorption with the light propagating along the *b* axis is suppressed by magnetic order. In particular, a spin-forbidden crystal-field transition shows a steep decrease in intensity upon the first-order phase transition from the spiral spin phase, AF2, to the low-temperature collinear spin phase, AF1. The large thermochroism makes it possible to visualize AF1 and AF2 domains, at the phase-coexistence state as a contrastive optical image. AF1 and the AF2 domains appear as stripes with a width of about 20–30 $\mu$m, implying relatively strong magnetic exchange interaction along a Mn zigzag chain (*c* axis).

DOI: 10.1103/PhysRevB.81.064406 PACS number(s): 75.80.+q, 75.60.Ch, 77.80.Dj, 78.20.−e

## I. INTRODUCTION

In recent years, magnetoelectric multiferroics, in which magnetic and ferroelectric (FE) orders coexist, have been intensively investigated.[1,2] In particular, the mutual coupling between the magnetic and FE orders in magnetoelectric multiferroics is of great interest.[3–16] The coupling can be enhanced if a magnetic domain wall is clamped to an FE domain wall[8,17,18] in multiferroic material. The motion of a composite domain wall which separates two regions with opposite magnetic and electric order parameters leads to a giant magnetoelectric response. Such clamping between a magnetic domain wall and an FE domain wall has been observed in some multiferroics by means of the imaging of second harmonic generation (SHG) of light.[19,20] A phase-coexistence state near a first-order phase boundary in a multiferroic material is another candidate that can enlarge the magnetoelectric response. If the application of a magnetic or an electric field can stimulate a motion of a domain wall dividing two regions with different phases, a large change in magnetic and electric polarizations should be induced. The dynamics of a domain wall between different order parameters or different magnetoelectric phases therefore stimulates much interest. A challenge for high-speed imaging of such spatial inhomogeneity by a simple method is indispensible for elucidating the domain-wall dynamics. Though the SHG imaging is a powerful tool from this viewpoint, it also suffers a disadvantage of rather long exposure time (approximately several minutes). In this study, we obtain a real-space image of a two-phase coexistence state in a magnetoelectric multiferroic $MnWO_4$ simply by using the light transmitted through a thin sample. The exposure time for the present imaging is as short as 50 ms. Hereafter, we use the term "domain" to refer to a region with a certain magnetoelectric phase, irrespective of the sign of the order parameter.[21] The domains of the spiral spin phase have been observed by diffraction techniques,[22,23] Lorentz electron microscopy,[24] and optical second harmonic generation method.[20]

$MnWO_4$ is a prototypical magnetoelectric multiferroics, in which the spiral spin structure and the FE polarization simultaneously appear.[9,25–27] $MnWO_4$ is crystallized in monoclinic structure ($P2/c$ with $\beta \sim 91°$), in which $Mn^{2+}$ ions surrounded by $O^{2-}$ octahedra are aligned in zigzag chains along the *c* axis. In this system, there are three long-wavelength magnetic ordering states, AF3, AF2, and AF1 at low temperatures.[28] The magnetic transition temperatures are ~13.5 K ($T_N$), ~12.7 K ($T_2$), and ~7.6 K ($T_1$), respectively. In AF1 ($T<T_1$) and AF3 ($T_2<T<T_N$), magnetic moments collinearly align in the *ac* plane forming an angle of about 35° with the *a* axis, whereas in AF2 ($T_1<T<T_2$), which is the spiral spin phase, an additional component along the *b* axis exists.[28] In $MnWO_4$, it has recently been reported that the FE single domain states in the spiral spin phase (AF2) is memorized even in the AF1 phase, which is the low-temperature paraelectric phase. As an explanation for this memory effect, the nuclei growth model of the FE embryos, which are the small polar nuclei of the AF2 phase with the spiral spin structure, is proposed.[25,29] In this model, the single domain state is reproduced across the first-order-type phase transition from the AF1 to the AF2 phase through the nuclei growth of the FE AF2 embryos in the AF1 phase. Taking account of this model, it is worthy to know how the spiral spin domains grow in the two-phase coexistence state, which appears upon the AF1-to-AF2 phase transition. Therefore, it is important to find the simple visualization technique of the domain with the spiral spin structure. In this study, we have found that optical absorption spectra show temperature dependence below the $T_N$. Utilizing the difference in the optical absorption coefficients between the paraelectric AF1 and the FE AF2 phases, a two-phase coexistence state has been visualized as a contrastive optical image. We have found that the FE-spiral spin domains appear as a stripe pattern perpendicular to the *a* axis in the two-phase coexistence state of the AF1 and the AF2 phase.

## II. EXPERIMENT

A single crystal of $MnWO_4$ was grown by the floating-zone method.[27] The crystal was oriented using Laue x-ray photographs and cleaved into a thin red plate with the widest surfaces of (010). The thickness (*t*) of the sample was about 200 $\mu$m, which was thin enough for optical transmission measurements below 2.7 eV. The optical principal axes in the visible region, which forms an angle of about 17° with the

 

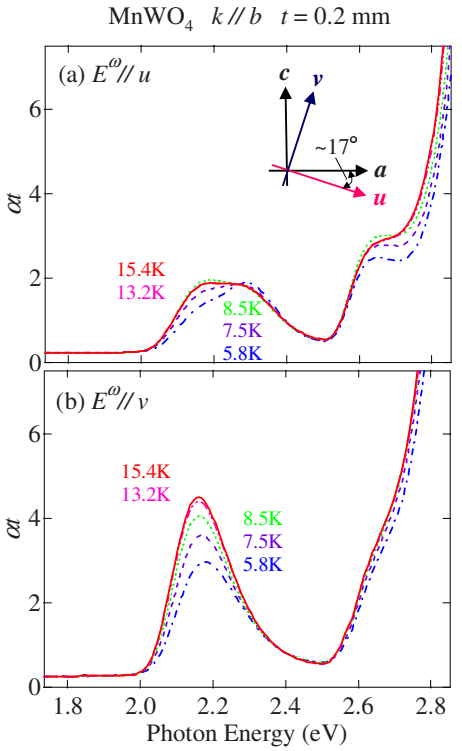


FIG. 1. (Color online) Optical absorption ($\alpha$) spectra with the light polarized along the (a) $u$ and (b) $v$ axes. The sample thickness $t$ is about 200 $\mu$m. Inset shows the relative configuration of the crystallographic axes, $a$ and $c$, and the optical principal axes, $u$ and $v$, within the $ac$ plane.

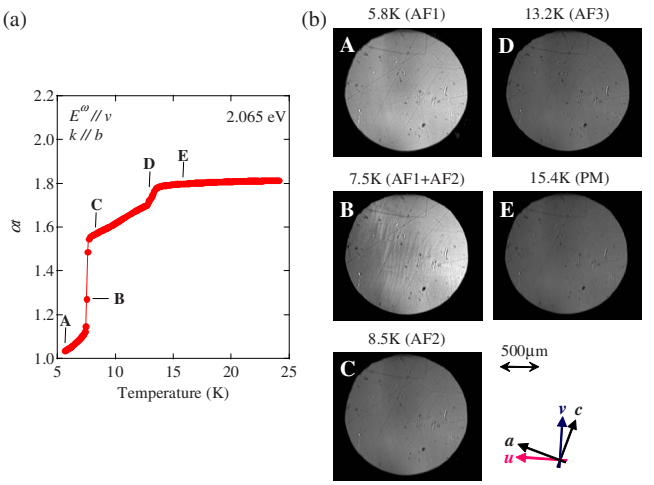


FIG. 2. (Color online) (a) Temperature dependence of the intensity of optical absorption of the 2.065 eV (600-nm) light polarized along the optical principal $v$ axis. (b) CCD images of the transmitted light at 2.065 eV. The horizontal and vertical axes are parallel to the $u$- and the $v$-optical principal axes, respectively. Each image was recorded at the temperature shown by A-E in (a). A, C, D, and E correspond to AF1, AF2, AF3, and PM phases, respectively. The image B is for a two-phase coexistence state of AF1 and AF2.

crystallographic axes within the $ac$ plane, were determined by the polarized microscope with crossed-Nicol configuration. In this paper, the two optical principal axes within the $ac$ plane are defined as $u$ and $v$ axes, respectively, as shown in the inset of Fig. 1(a). It was confirmed that the optical principal axes little change with cooling down to the AF1 phase. The sample was mounted on a copper holder in a $^4$He closed-cycle refrigerator. Optical absorption spectra for the photon energies ranging from 1.5 to 3 eV were measured with the linearly polarized light propagating along the $b$ axis. The intensity of the transmitted light was detected by using a photodiode or a charge-coupled device (CCD) camera.

## III. RESULTS AND DISCUSSION

Figures 1(a) and 1(b) display the optical absorption spectra for the light polarized parallel to the $u$ and $v$ axes, respectively, at various temperatures. A steep increase in optical absorption above 2.7 eV for both light polarizations likely corresponds to the onset of an interatomic transition between O $2p$ and Mn $3d$ levels.[30] Below the charge-transfer transition, some broad peaks are observed around 2.0–2.4 eV and 2.65 eV. Judging from the intensities and positions of the peaks, they should be assigned to intra-atomic spin-forbidden crystal-field transitions between different $3d$ orbitals of a $Mn^{2+}$ ion.[31–33] Comparing the observed spectra of $MnWO_4$ with that reported in MnO, the lower energy bands around 2.0–2.4 eV correspond to the transition from $^6A_{1g}$ to $^4T_{1g}$, and the higher band at 2.65 eV should be ascribed to the $^6A_{1g}$ to $^4T_{2g}$ transition in an octahedral crystal field.[34] Since the site symmetry at each $Mn^{2+}$ ion is monoclinic ($C_2$) in $MnWO_4$, the degeneracy of the excited states should be lifted. Both $^4T_{1g}$ and $^4T_{2g}$ should be split into three states, which are composed of one $^4A$ and two $^4B$ states. The splitting band structure around 2.0–2.4 eV in Fig. 1(a) would hence reflect the level split of the excited states $^4T_{1g}$ to $^4A + 2\,^4B$.

The intensity of the peak centered around 2.15 eV decreases below $T_N \sim 13.5$ K, irrespective of the polarization of light. A shoulder at 2.65 eV for $E^w \| u$ exhibits a similar tendency. The absorption at 2.3 eV for $E^w \| u$, however, shows converse temperature dependence. In Fig. 2(a), the temperature dependence of the lowest-energy optical absorption with the light polarized along the $v$ axis is displayed. Here the measurements were performed at 2.065 eV, where the transmitted light intensity is stronger than the peak energy. Three anomalies are found at the three magnetic transition temperatures. In particular, a sudden decrease in the optical absorption is observed at the phase transition from AF2 to AF1. Figure 2(b) shows a CCD image of the transmitted light at 2.065 eV polarized along the $v$ axis for each magnetic phase. Reflecting the change in optical absorption shown in Fig. 2(a), the CCD image becomes brighter, as decreasing temperature from the paramagnetic (PM) to the AF1 phase. In particular, the brightness of the image remarkably changes with the transition from the AF2 phase (C) to the AF1 phase (A). Since the phase transition between AF1 and AF2 is of first order, a two-phase coexistence state should be expected around $T_1$ (B).[27] Taking advantage of the difference in the transmission of light intensity between AF1 and AF2, the coexistence state of the AF1 and the AF2 phases may be visualized as reported in another antiferro-

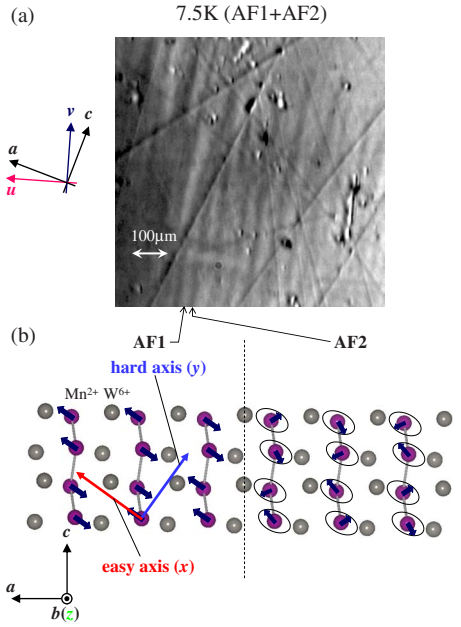


FIG. 3. (Color online) (a) CCD image B in Fig. 2(b) with a higher contrast. (b) Schematic of a domain boundary between the AF1 and the AF2 phases. The crystallographic $a$, $b$, and $c$ as well as the orthogonal magnetic principal axes, which are easy ($x$), hard ($y$), and $z$ axes, are shown.

magnetic material.[35] In fact, one can see a stripe structure only in the image B in Fig. 2(b).

Figure 3(a) presents the CCD image B (7.5 K) in Fig. 2(b) in a magnified scale. The stripe pattern should be due to domain structures of the two-phase coexistence state. The darker regions are the AF2 domains with the spiral spin structure and the brighter regions are the AF1 domains with the collinear spin structure since the absorption of 2.065 eV photons is larger in the AF2 phase than in the AF1 phase as shown in Fig. 2. The stripes run approximately perpendicular to the $a$ axis as displayed in Fig. 3(a). The typical width of domain stripes is about 20–30 $\mu$m. This stripe contrast indicates that the AF1 and AF2 domains are in the sticklike or platelike shapes. Although we can observe the gradual contrast induced by the inhomogeneity of heat flow within the samples in A and C of Fig. 2(b), the stripe-contrast distribution in image B is different from that observed in other phase. The origin of the stripe contrast would be ascribed to a different factor from heat inhomogeneity. Since the $Mn^{2+}$ layers are intervened by the $W^{6+}$ layer along the $a$ axis as displayed in Fig. 3(b), the magnetic exchange interaction along the $a$ axis may be weaker than that along the Mn zigzag chain parallel to the $c$ axis. Therefore, one possible origin of the observed stripe pattern would be an anisotropic exchange interaction.

Finally, let us discuss the origin of the difference in absorption intensity between AF1 and AF2. Although spin-lattice coupling exists in this system,[9,27] the atomic displacement induced by the successive phase transition in the low temperature should be too small to directly affect the observed optical absorption behavior. The large thermochromism, which makes it possible to visualize the two-phase coexistence state, could be induced by the difference

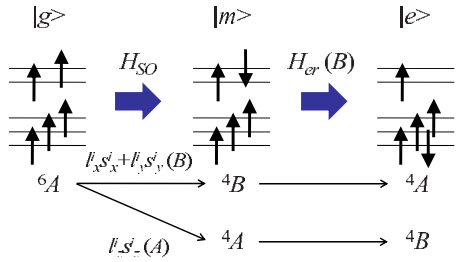


FIG. 4. (Color online) Schematic electronic-level diagram of the transition around 2.0–2.4 eV. The transition process, which is represented by the matrix element $\langle e|H_{er}|m\rangle\langle m|H_{SO}|g\rangle$, is shown.

in the magnetic structure. Since the crystal-field transition for a $Mn^{2+}$ ion with the high-spin $3d^5$ configuration is forbidden by the spin selection rule, the spin-orbit interaction, which couples the sextet ground state ($^6A$) with the quartet exited state ($^4A$, $^4B$), should be considered in the crystal-field transition process. A possible transition-matrix element, which contains the spin-orbit interaction $H_{SO}$, is described as $\langle e|H_{er}|m\rangle\langle m|H_{SO}|g\rangle$, in which $e$, $m$, and $g$ represent the excited state, an intermediate state and the ground state, respectively[36] (see Fig. 4). The $\langle e|H_{er}|m\rangle$ term expresses an electric or a magnetic dipole transition from the $|m\rangle$ to $|e\rangle$ state in the $3d$-electron system. $H_{SO}$ is given by $H_{SO}=\Sigma_i \xi_i \boldsymbol{l}_i \cdot \boldsymbol{s}_i$, where $\boldsymbol{l}_i$ and $\boldsymbol{s}_i$ are the orbital- and spin-momentum operators of the $i$th electron, respectively. $\xi_i$ denotes the spin-orbit coupling constant of the $i$th electron. In the magnetic principal axes setting [see Fig. 3(b)],[37] $H_{SO}$ is represented as $H_{SO}=\Sigma_i \xi_i (l^i_x s^i_x + l^i_y s^i_y + l^i_z s^i_z)$. Since the irreducible representation of $l^i_x s^i_x + l^i_y s^i_y$ is $B$ and that of $l^i_z s^i_z$ is $A$ in the $C_2$ site symmetry, the intermediate states ($m$) coupled with the ground state ($^6A$) by the spin-orbit coupling terms $l^i_x s^i_x + l^i_y s^i_y$ and $l^i_z s^i_z$ become $^4B$ and $^4A$, respectively. One should note here that the ground state ($^6A$) of each $Mn^{2+}$ ion does not have the sixfold degeneracy in the magnetic order phases. The ground state of every $Mn^{2+}$ ion in the AF1 phase is approximately represented as $|g\rangle=|^6A; S_x=\pm 5/2\rangle$. Taking account that the operator $l^i_x s^i_x$ does not change the $S_x$ value, $\langle {}^4B|l^i_x s^i_x|g\rangle=0$, for the AF1 phase. This selection rule partly relaxes in the spin-spiral AF2 phase. For example, the ground state of the $Mn^{2+}$ ion with a spin parallel to the $z$ ($b$) axis, which appears in AF2 phase, can be approximately described as $|g\rangle=|^6A; S_z=\pm 5/2\rangle$. Now, the matrix element $\langle {}^4B; S_z=\pm 3/2|l^i_x s^i_x|g\rangle$ is not zero.[38] In contrast, the matrix element $\langle {}^4B|l^i_y s^i_y|g\rangle$ does not show such a clear difference between AF1 and AF2. A dipole transition from $|g\rangle$ to an excited state may exhibit a sudden change in intensity upon the phase transition from AF2 to AF1 because the second term of the amplitude $\langle e|H_{er}|{}^4B\rangle\langle {}^4B|\Sigma_i \xi_i (l^i_x s^i_x + l^i_y s^i_y)|g\rangle$ is largely influenced by the $S_x$ and $S_z$ value of $|g\rangle$, as mentioned above. As a result, the sudden decrease in the optical absorption across the phase transition from the AF2 to the AF1 phase should be ascribed to the spin-orbit transition process, which contains $\langle {}^4B|\Sigma_i \xi_i l^i_x s^i_x|g\rangle$. Since the irreducible representation of the electric or the magnetic dipole process for the light polarized in the $xy$ plane is $B$, the absorption band at 2.15 eV as well as 2.65 eV can be assigned to the crystal-field transitions from $^6A$ to $^4A$. The intensity of an optical

transition from $^6A$ to $^4B$ should have inverse temperature dependence upon the magnetic transition from AF2 to AF1. In this transition, the matrix element contains the $l_z^i s_z^i$ term as $\langle e|H_{er}|^4A\rangle\langle^4A|\Sigma_i \xi_i l_z^i s_z^i|g\rangle$. When the spin moment is parallel to the $z$ ($b$) axis, this matrix element should vanish. As a consequence, the absorption with the electron excitation to a state $^4B$ should increase in intensity in the AF1 phase, where all the $Mn^{2+}$ moments are perpendicular to the $z$ axis. A hump at 2.3 eV in Fig. 1(a) can be assigned to such an excitation.

## IV. SUMMARY

In summary, we have found that the optical absorption spectra of $MnWO_4$ are dependent on the magnetic structure. In particular, it is found that the lowest-energy spin-forbidden crystal-field transition shows a sudden decrease in intensity in the collinear spin phase, AF1. We have shown that magnetic order plays a key role of the observed optical absorption change. It is demonstrated that the two-phase coexistence state of the AF1 phase with the collinear spin structure and the AF2 phase with the spiral spin structure is visualized as a sharp contrast in the brightness in the optical image through the difference in the optical absorption between the AF1 and the AF2 phase at the spin-forbidden-type crystal-field transition. The observed image with a stripe pattern indicates that the spiral spin domains first grow as a sticklike or platelike shape perpendicular to the $a$ axis, along which the $Mn^{2+}$ layers are intervened by $W^{6+}$ layer. The exposure time as short as 50 ms will be applicable to the investigation of the dynamics of the magnetic and electric domain walls.

## ACKNOWLEDGMENTS

We thank Woo Seok Choi, Y. S. Lee, and T. W. Noh for the collaboration in the early stage of this study. This work was supported in part by a Grant-in-Aid for Scientific Research (Grant No. 21740237 and No. 19052001) from MEXT, Japan and the Asahi Glass Foundation.

*Present address: Department of Advanced Materials, University of Tokyo, Kashiwa 277-8561, Japan.

[1] M. Fiebig, J. Phys. D **38**, R123 (2005).
[2] S.-W. Cheong and M. Mostovoy, Nature Mater. **6**, 13 (2007).
[3] T. Kimura, T. Goto, H. Shintani, K. Ishizaka, T. Arima, and Y. Tokura, Nature (London) **426**, 55 (2003).
[4] N. Hur, S. Park, P. A. Sharma, J. S. Ahn, S. Guha, and S.-W. Cheong, Nature (London) **429**, 392 (2004).
[5] T. Lottermoser, T. Lonkai, U. Amann, D. Hohlwein, J. Ihringer, and M. Fiebig, Nature (London) **430**, 541 (2004).
[6] T. Kimura, G. Lawes, and A. P. Ramirez, Phys. Rev. Lett. **94**, 137201 (2005).
[7] G. Lawes, A. B. Harris, T. Kimura, N. Rogado, R. J. Cava, A. Aharony, O. Entin-Wohlman, T. Yildrim, M. Kenzelmann, C. Broholm, and A. P. Ramirez, Phys. Rev. Lett. **95**, 087205 (2005).
[8] Y. Yamasaki, S. Miyasaka, Y. Kaneko, J.-P. He, T. Arima, and Y. Tokura, Phys. Rev. Lett. **96**, 207204 (2006).
[9] K. Taniguchi, N. Abe, T. Takenobu, Y. Iwasa, and T. Arima, Phys. Rev. Lett. **97**, 097203 (2006).
[10] S. Park, Y. J. Choi, C. L. Zhang, and S.-W. Cheong, Phys. Rev. Lett. **98**, 057601 (2007).
[11] M. Kenzelmann, G. Lawes, A. B. Harris, G. Gasparovic, C. Broholm, A. P. Ramirez, G. A. Jorge, M. Jaime, S. Park, Q. Huang, A. Ya. Shapiro, and L. A. Demianets, Phys. Rev. Lett. **98**, 267205 (2007).
[12] Y. J. Choi, H. T. Yi, S. Lee, Q. Huang, V. Kiryukhin, and S.-W. Cheong, Phys. Rev. Lett. **100**, 047601 (2008).
[13] T. Kimura, Y. Sekio, H. Nakamura, T. Siegrist, and A. P. Ramirez, Nature Mater. **7**, 291 (2008).
[14] K. Taniguchi, N. Abe, S. Ohtani, H. Umetsu, and T. Arima, Appl. Phys. Express **1**, 031301 (2008).
[15] S. Ishiwata, Y. Taguchi, H. Murakawa, Y. Onose, and Y. Tokura, Science **319**, 1643 (2008).
[16] S. Seki, Y. Onose, and Y. Tokura, Phys. Rev. Lett. **101**, 067204 (2008).
[17] F. Kagawa, M. Mochizuki, Y. Onose, H. Murakawa, Y. Kaneko, N. Furukawa, and Y. Tokura, Phys. Rev. Lett. **102**, 057604 (2009).
[18] Y. Tokunaga, N. Furukawa, H. Sakai, Y. Taguchi, T. Arima, and Y. Tokura, Nature Mater. **8**, 558 (2009).
[19] M. Fiebig, T. Lottermoser, D. Fröhlich, A. V. Goltsev, and R. V. Pisarev, Nature (London) **419**, 818 (2002).
[20] D. Meier, M. Maringer, T. Lottermoser, P. Becker, L. Bohatý, and M. Fiebig, Phys. Rev. Lett. **102**, 107202 (2009).
[21] It is conventional to use the term "domain" for the regions with a different orientation of order parameter within one phase of ferromagnetic or ferroelectric materials. On the other hand, we can find the usage of the term domain for each separated area in the two-phase coexisting state of antiferromagnetic or multiferroic materials: Refs. 17 and 35. In this paper, we employ the latter usage of the term domain.
[22] S. B. Palmer, J. Baruchel, A. Drillat, C. Patterson, and D. Fort, J. Magn. Magn. Mater. **54-57**, 1626 (1986).
[23] J. C. Lang, D. R. Lee, D. Haskel, and G. Srajer, J. Appl. Phys. **95**, 6537 (2004).
[24] M. Uchida, Y. Onose, Y. Matsui, and Y. Tokura, Science **311**, 359 (2006).
[25] A. H. Arkenbout, T. T. M. Palstra, T. Siegrist, and T. Kimura, Phys. Rev. B **74**, 184431 (2006).
[26] O. Heyer, N. Hollmann, I. Klassen, S. Jodlauk, L. Bohatý, P. Becker, J. A. Mydosh, T. Lorenz, and D. Khomskii, J. Phys.: Condens. Matter **18**, L471 (2006).
[27] K. Taniguchi, N. Abe, H. Sagayama, S. Otani, T. Takenobu, Y. Iwasa, and T. Arima, Phys. Rev. B **77**, 064408 (2008).
[28] G. Lautenschläger, H. Weitzel, T. Vogt, R. Hock, A. Böhm, M. Bonnet, and H. Fuess, Phys. Rev. B **48**, 6087 (1993).
[29] K. Taniguchi, N. Abe, S. Ohtani, and T. Arima, Phys. Rev. Lett. **102**, 147201 (2009).
[30] A. Nogami, T. Suzuki, and T. Katsufuji, J. Phys. Soc. Jpn. **77**,

115001 (2008).

[31] N. N. Kovaleva, A. V. Boris, C. Bernhard, A. Kulakov, A. Pimenov, A. M. Balbashov, G. Khaliullin, and B. Keimer, Phys. Rev. Lett. **93**, 147204 (2004).

[32] S. Sugano, Y. Tanabe, and H. Kamimura, *Multiplets of Transition Metal Ions in Crystals* (Academic, New York, 1970), p. 106.

[33] The interionic *d-d* transition between neighboring $Mn^{2+}$ is another possible origin of the observed peak as reported in Ref. 31. However, we cannot explain temperature dependence of the observed peak intensity by the interionic transition. In AF1 with commensurate collinear-spin structure, an electron can only transfer to the half of the neighboring $Mn^{2+}$ sites within *ac* plane because of the Pauli's exclusion principle. On the other hand, in the spiral spin phase (AF2), in which the neighboring spin angle is about 90°, transition probability to the neighboring sites becomes half of that in AF1, although an electron can transfer to the all neighboring sites. As a result, transition probability should hardly be affected by the spin structure change from AF1 to AF2. In addition, we cannot explain the observed optical principal-axes directions, which deviate from the *a* and the *c* axes, although the optical principal axes within the *ac* plane should reflect the zigzag-chain direction in the interionic transition.

[34] D. R. Huffman, R. L. Wild, and M. Shinmei, J. Chem. Phys. **50**, 4092 (1969).

[35] A. R. King and D. Paquette, Phys. Rev. Lett. **30**, 662 (1973).

[36] As for the other possible matrix element $\langle e|H_{SO}|m\rangle\langle m|H_{er}|g\rangle$, an almost similar discussion can be made.

[37] In this study, we define the magnetic principal axes within the *ac* plane as the easy ($x$) and the hard ($y$) axis, respectively. In this magnetic principal-axes setting, the crystallographic $b$ axis is defined as $z$ axis.

[38] For example, we consider addition of spin angular momentum between the first electron spin $s_1(=1/2)$ and the other spin $s_o(=2)$, in which the moments of the rest four spins are added. In AF2, the ground state for one of the two $Mn^{2+}$ sites is represented as $|g\rangle=|S=5/2,S_z=\pm 5/2\rangle=|s_{1z}=\pm 1/2,s_{oz}=\pm 2\rangle$. Since $s_x=1/2(s_++s_-)$ for $z$ axis as the quantization axis, $s_x^1|g\rangle=c_0|s_{1z}=\mp 1/2,s_{oz}=\pm 2\rangle=c_1|S=5/2,S_z=\pm 3/2\rangle+c_2|S=3/2,S_z=\pm 3/2\rangle$. $c_0$, $c_1$ and $c_2$ are constants. On the other hand, $s_x^1|g\rangle=\pm\hbar/2|g\rangle$ for another $Mn^{2+}$ site, in which $|g\rangle=|S=5/2,S_x=\pm 5/2\rangle$. In this case, the state with $S=3/2$ is not hybridized through the spin-orbit coupling.